Upper mantle structure beneath the Dinarides and the Alps from surface wave tomography

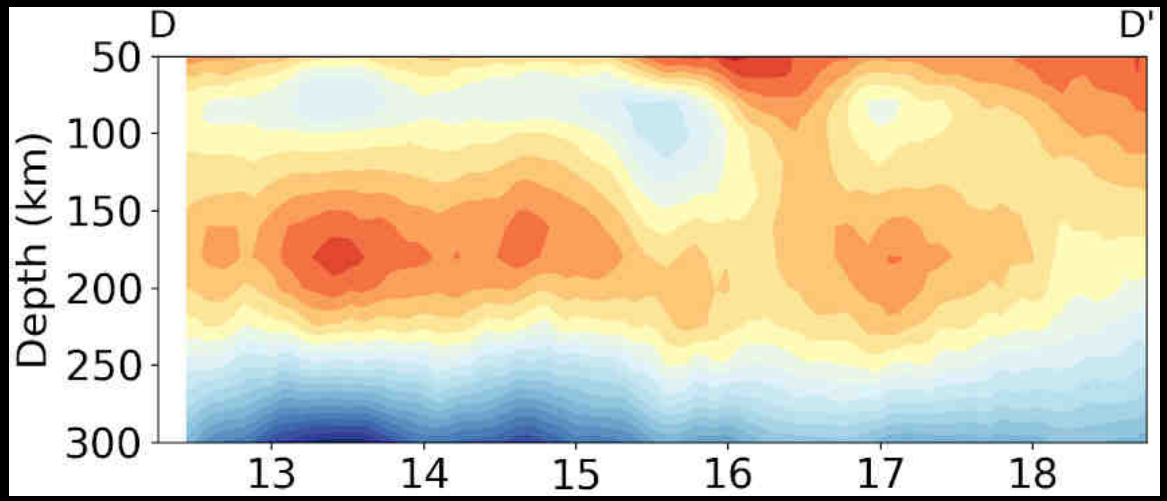

Petr Kolínský[1], Tena Belinić[2], Josip Stipčević[3], Irene Bianchi[1], Florian Fuchs[1], Götz Bokelmann[1] and the AlpArray Working Group[4]

(1) Department of Meteorology and Geophysics, University of Vienna, Austria
(2) KrakenSystems Ltd, Zagreb, Croatia
(3) Department of Geophysics, University of Zagreb, Croatia
(4) www.alparray.ethz.ch

EGU General Assembly 2020 online activities “Sharing Geoscience Online”, Thursday, 7. May, 2020

© Authors. All rights reserved

part 1: Dinarides

© Authors. All rights reserved

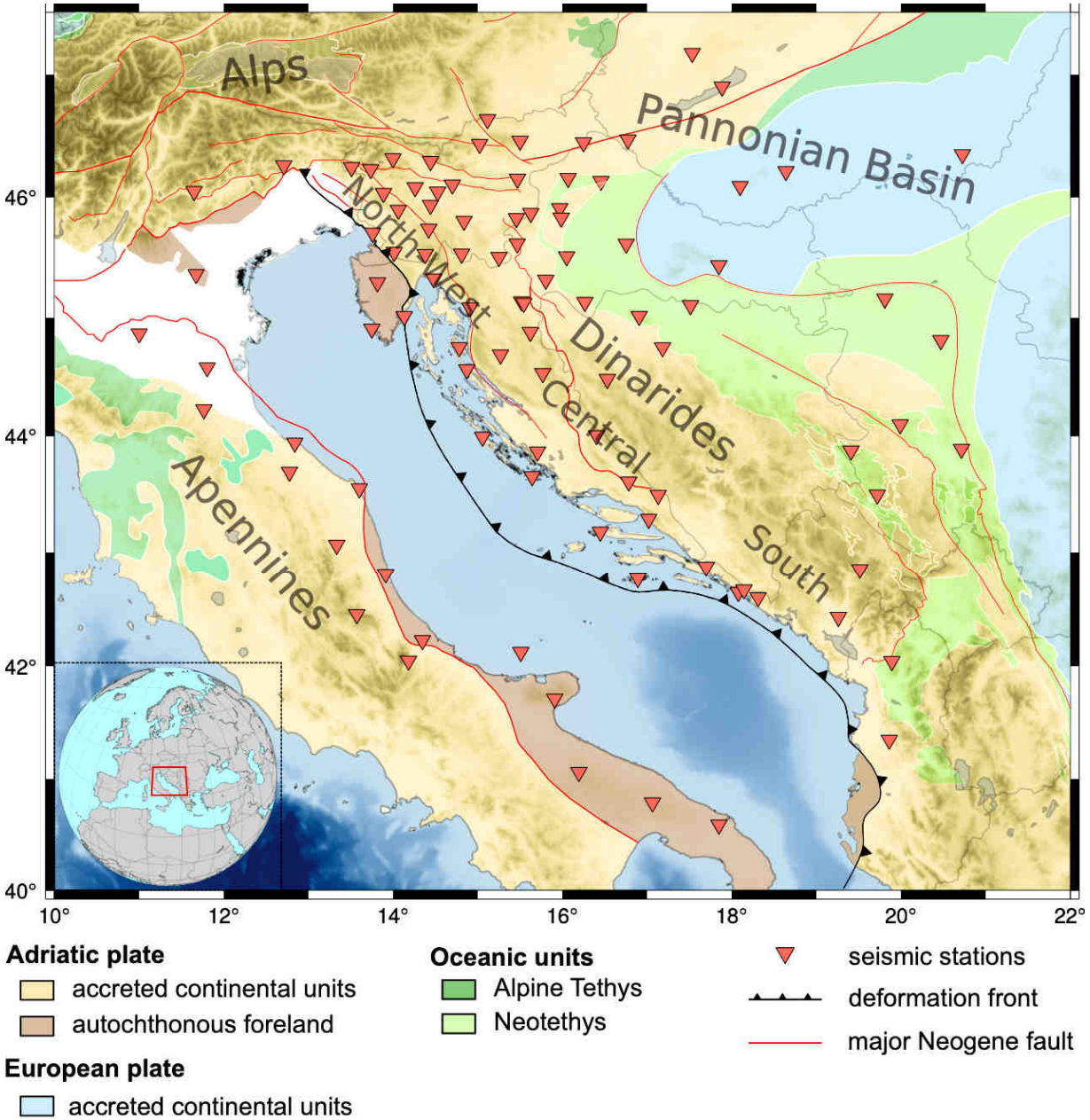

Map of seismic stations used in this study (red triangles) overlaid on the regional tectonic map (modified from Schmid et al., 2008). Solid red lines represent main Tertiary faults, while the black barbed line defines the current orogenic front on the east Adriatic side.

© Authors. All rights reserved

Abstract

To investigate the Dinaric mantle structure, we use regional-to-teleseismic surface-wave records from 98 seismic stations in the wider Dinarides region to create a 3D shear-wave velocity model. Two-station method is used to extract Rayleigh-wave phase velocity while tomography and 1D inversion of the phase velocity are employed to map the depth dependent shear-wave velocity. Resulting velocity model reveals a robust high-velocity anomaly present under the whole Dinarides, reaching the depths of 160 km in the north to more than 200 km under southern Dinarides. These results do not agree with most of the previous investigations and show continuous underthrusting of the Adriatic lithosphere under Europe along the whole Dinaric region. The geometry of the down-going slab varies from the deeper slab in north and south to the shallower underthrusting in the center. On-top of both north and south slabs there is a low-velocity wedge indicating lithospheric delamination and slab rollback which could explain the 200 km deep highvelocity body existing under the southern Dinarides.

a)

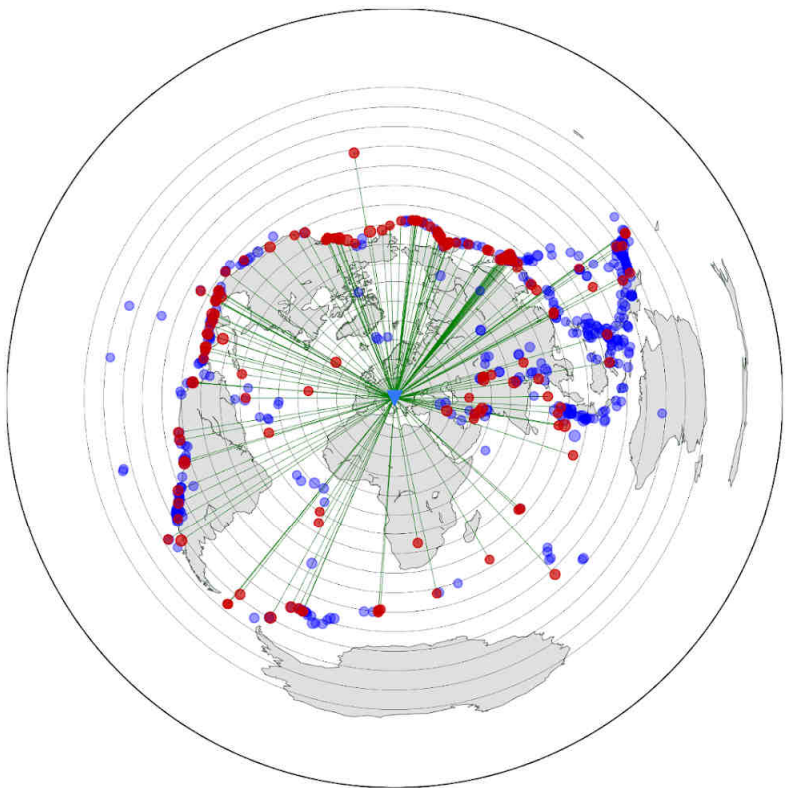

b)

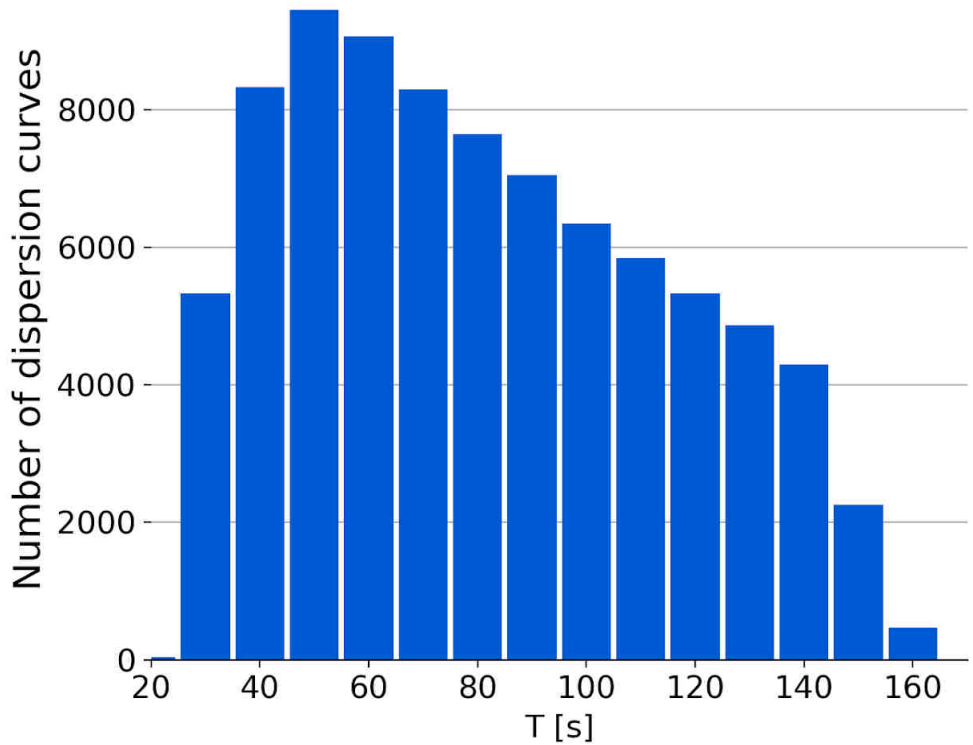

a) Map of 151 earthquake locations used in this study (red dots mark used events, blue dots mark rejected events). Green lines are great circle paths, grey circles are n*1000 km distances and blue triangle marks the investigated region. Earthquakes are selected from 2010 – 2018.

b) Histogram of the number of good phase dispersion curves per period after applying the traveltime and smoothness criteria. The period range of measurement is 30 – 160 s. We use both vertical and radial components to extract Rayleigh wave phase velocity dispersion curves.

© Authors. All rights reserved

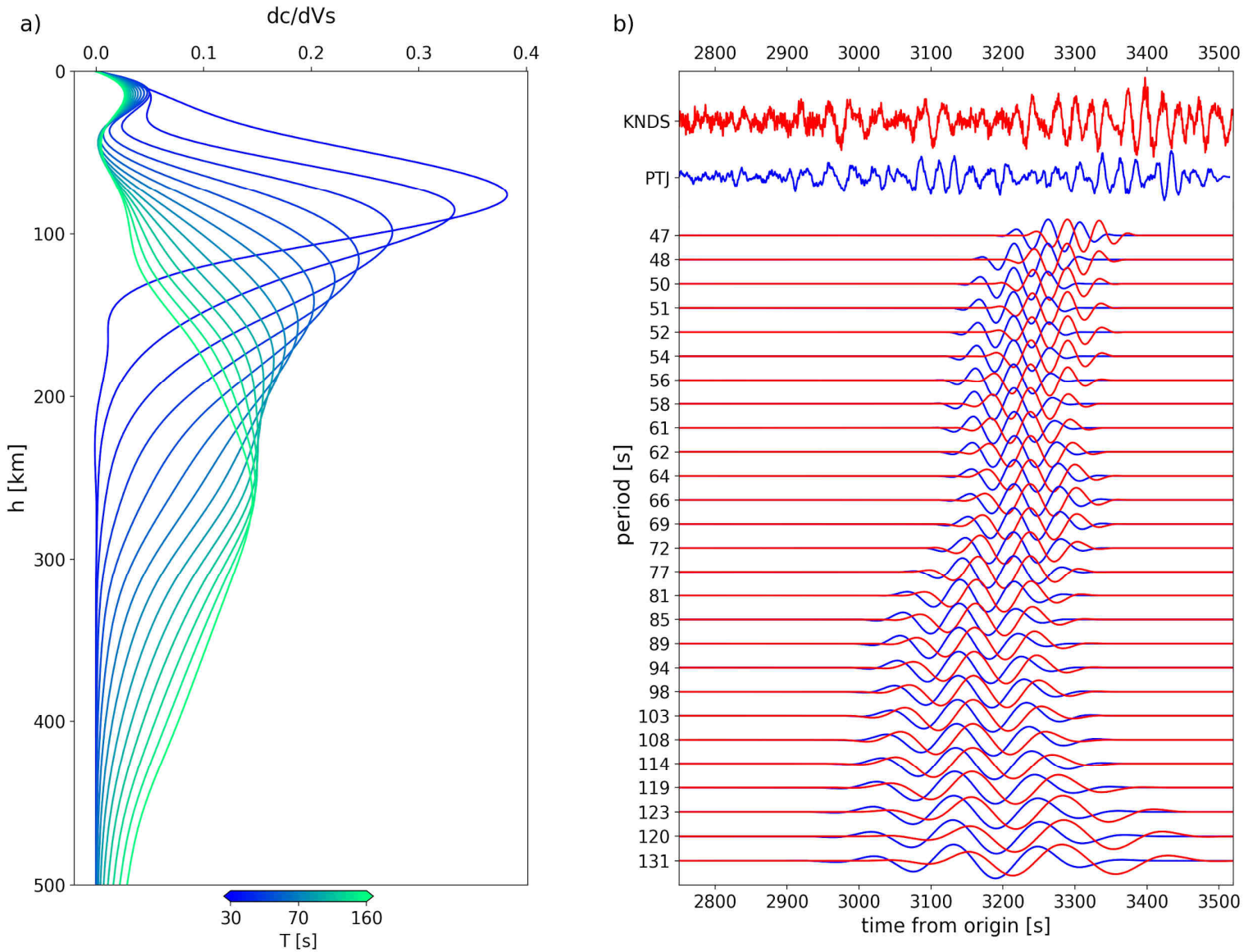

a) Depth sensitivity kernels for model ak135 of the Rayleigh wave for periods between 30 and 160 s.

b) Quasi-harmonic signals of the event that occurred on 2018 May 5 at 06:19:05 GMT near the Philippines. The blue traces are recorded at the station PTJ and the red ones at the station KNDS. Top panel shows raw seismograms. Central panel shows 27 traces bandpass filtered in the frequency domain at the periods shown on the left side and tapered in the time domain around the arrival time of the fundamental mode.

© Authors. All rights reserved

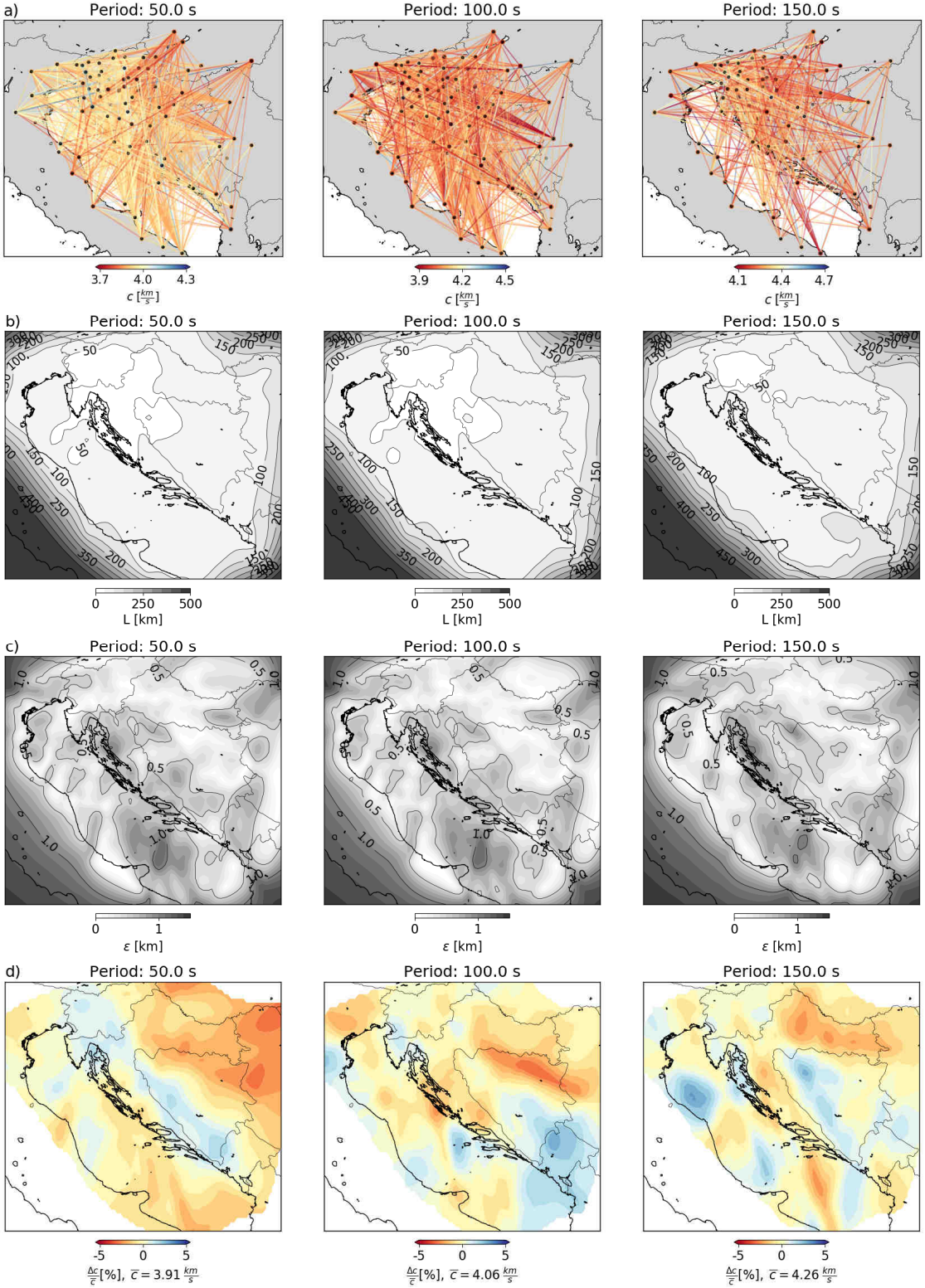

Tomography including resolution estimates is provided for various frequencies using the method and code by Yanovskaya and Ditmar (1990). Local dispersion curves are inverted for depths from the surface down to 300 km.

For periods of 50, 100 and 150 s:

a) the interstation path velocities (color marks velocity);

b) and c) the resolution maps i.e. averaging area and the stretching factor calculated following Yanovskaya and Ditmar (1990);

d) the phase velocity maps (only for areas with resolution L < 150 km).

© Authors. All rights reserved

Example of the 1D phase velocity inversion for three different locations. Blue stars mark the location while the blue dots indicate the phase velocities taken at each location from the phase velocity maps. Red line in the same image is the dispersion curve of the final mean model with the variations between minimum and maximum velocity in grey.

The rightmost panel shows the final mean shear-wave velocity structure (red line) obtained after 30 inversions. Grey area represents the standard deviation for each layer.

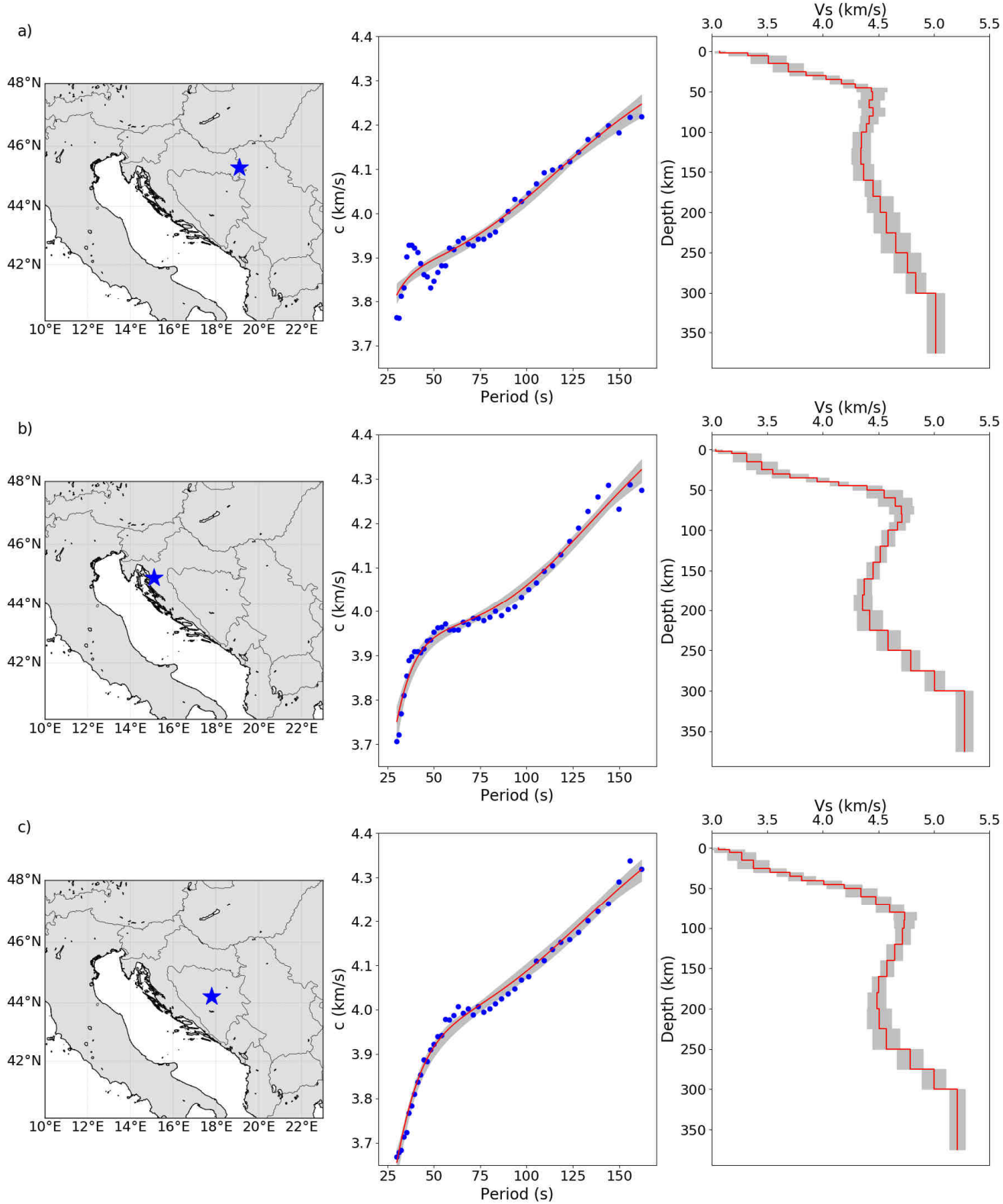

© Authors. All rights reserved

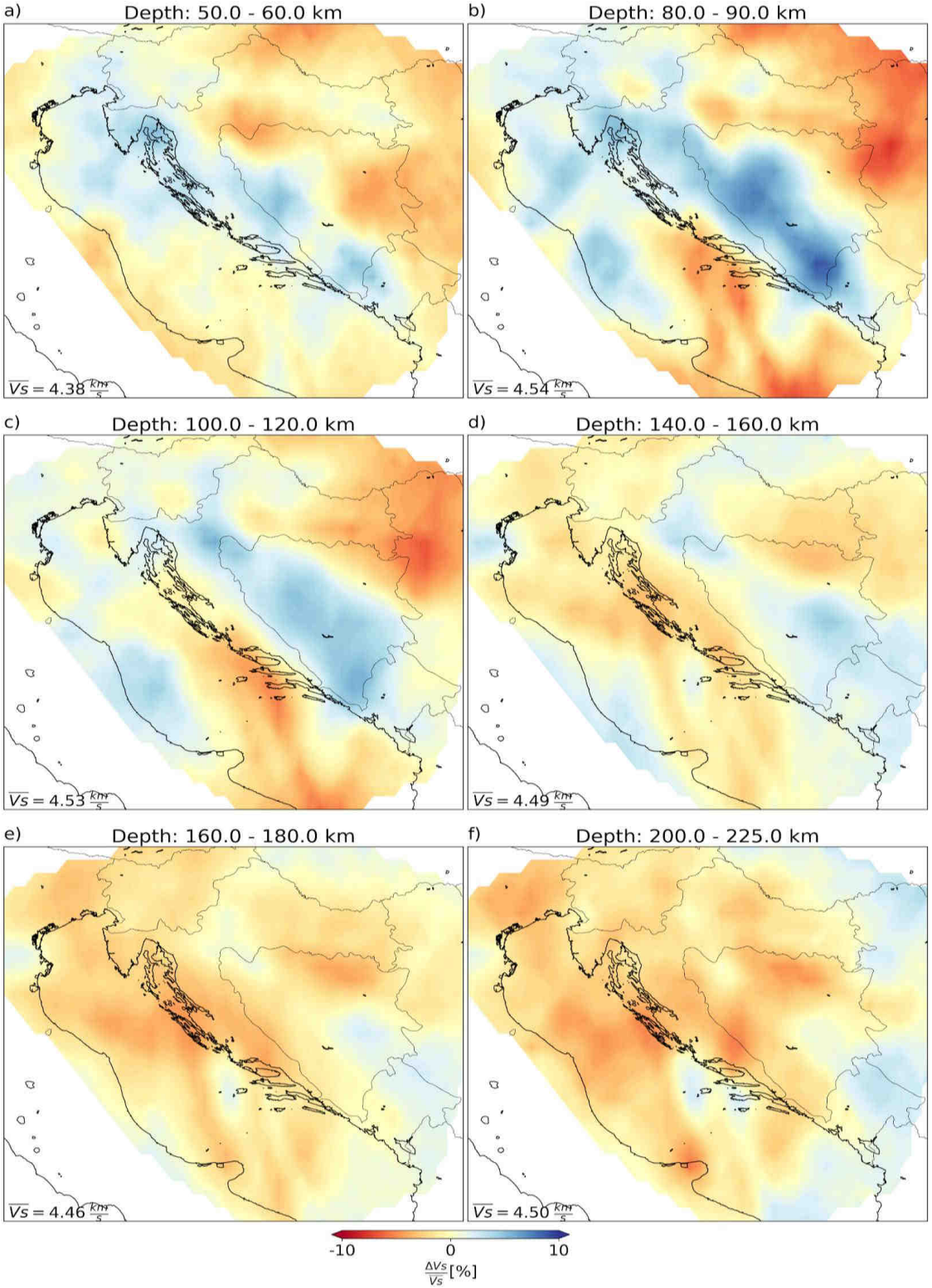

Maps of the shear wave velocity model obtained after the inversion of phase velocity dispersion curves for layers at depths: 50-60, 80-90, 100-120, 140-160, 160-180 and 200-225 km.

© Authors. All rights reserved

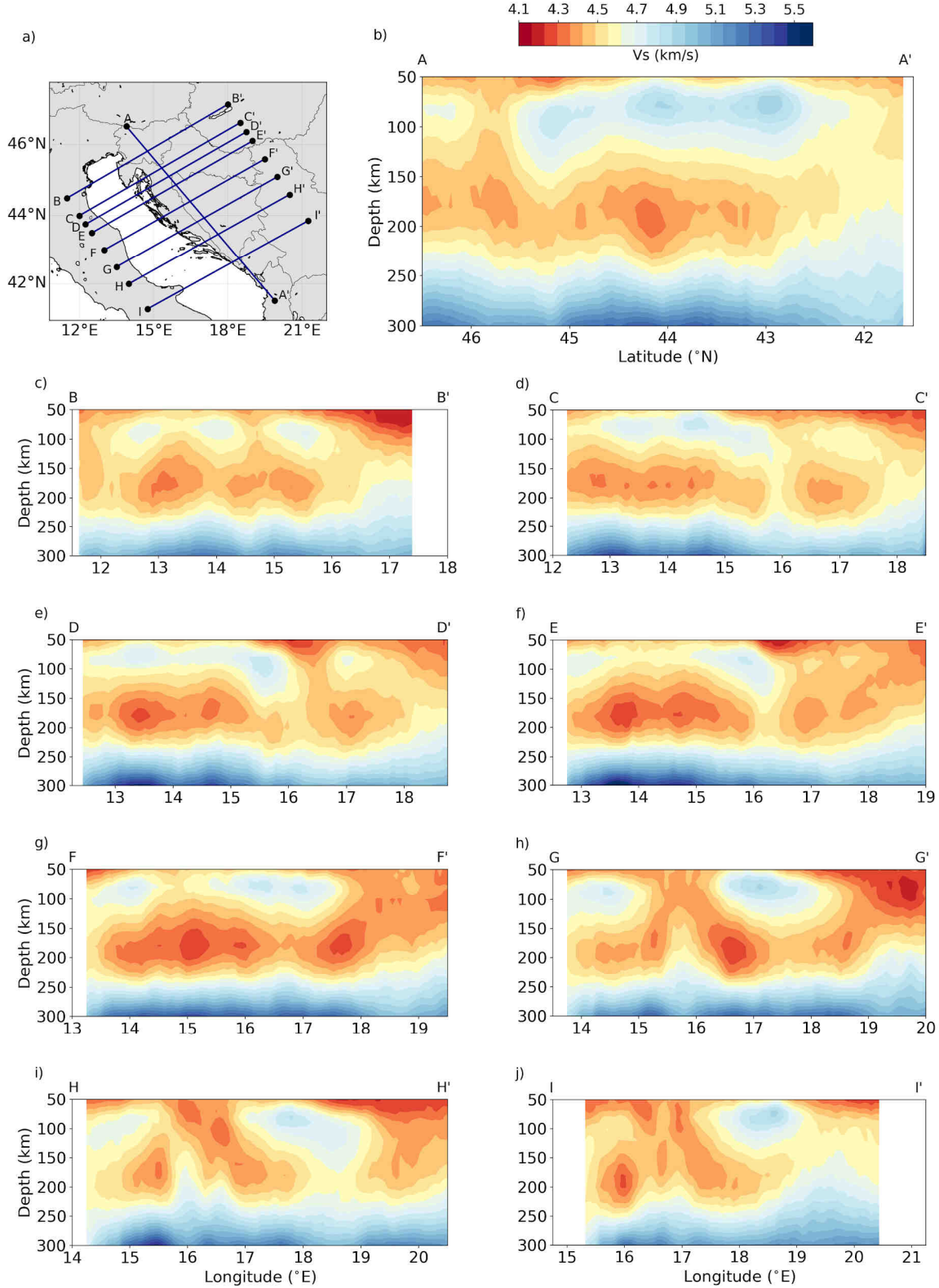

Cross-sections through the shear wave velocity model.

a) Location of the cross-sections shown in this figure. Please note that the depth of each profile starts at 50 km as we excluded the uppermost part where the surface waves have low sensitivity.

Panel b) shows the shear velocity versus depth in the upper mantle along the profile parallel to the Dinarides.

Panels c) through j) show the shear velocity versus depth in the upper mantle along the profiles crossing the Dinarides.

© Authors. All rights reserved

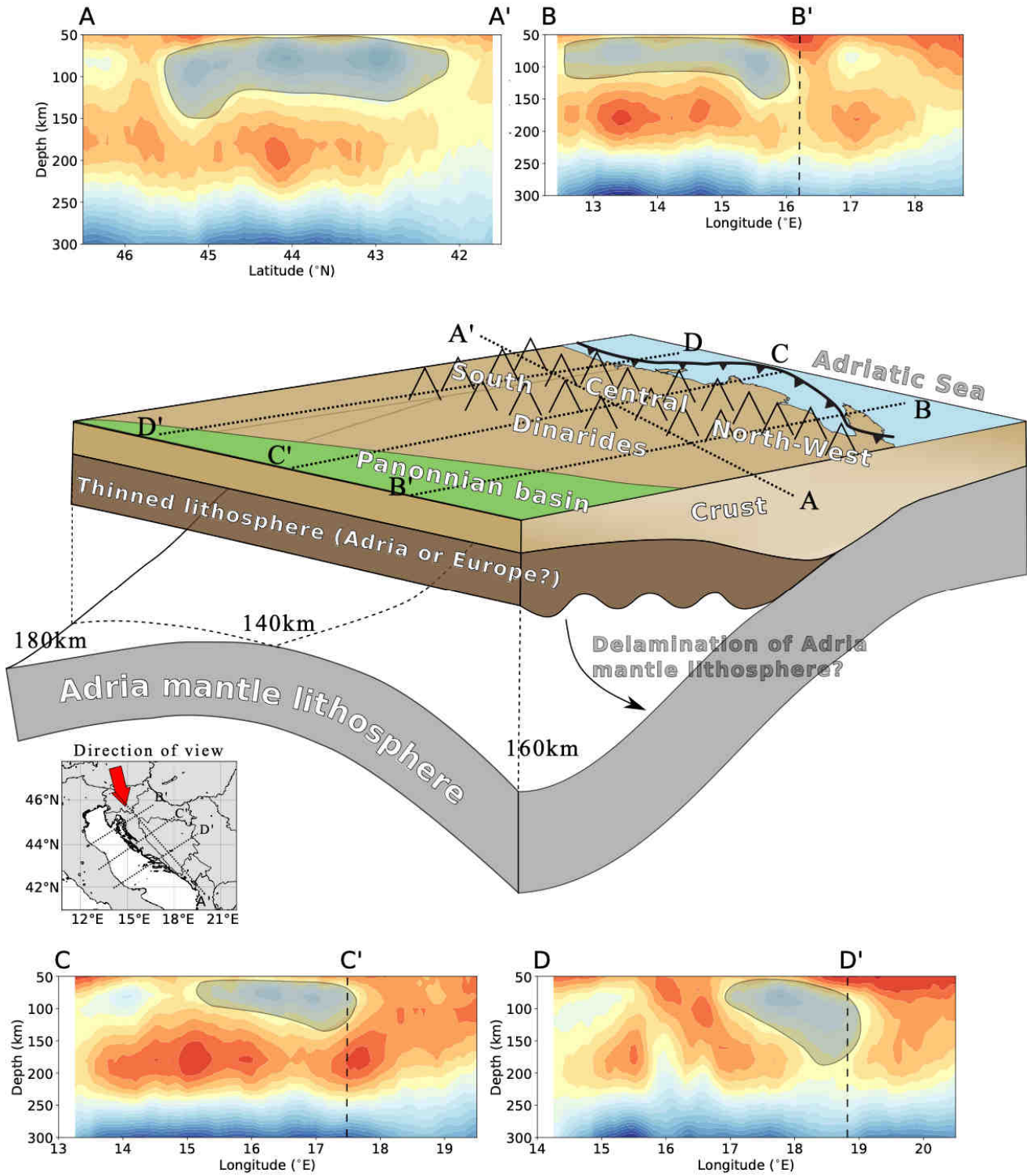

Schematic interpretation of the Dinarides lithospheric structure (not to scale) from the new 3-D shear-wave velocity model.

Subimages a) to d) are the cross-sections through the new shear-wave velocity model with shaded areas marking the location and shape of the underthrusting Adriatic lithosphere (depth section starts at 50 km).

Markings AA', BB', CC' and DD' denote the extent of interpreted part of each cross-section in the main tectonic sketch. The locations of the cross-sections along with the view angle of the tectonic sketch are shown in small subimage in the left corner of the central panel.

Tectonic sketch in the central image depicts the subducted Adria lithosphere beneath the Dinarides. The depth, extent and the geometry of the sub-ducted lithosphere varies from north to south suggesting different mechanism of slab creation. Dark brown color de-notes the thinned lithosphere of un-certain origin, either thermo-chemically thinned European or possibly Adriatic, thinned due to the delamination.

© Authors. All rights reserved

part 2: Alps

(work in progress)

© Authors. All rights reserved

Abstract

The AlpArray seismic network stretches hundreds of kilometers in width and more than thousand kilometers in length. It is distributed over the greater Alpine region (Europe) and consists of around 250 temporary and around 400 permanent broadband stations with interstation distances around 40 km. The earthquakes are selected from years 2016-2019.

We use two-station phase velocities measured from teleseismic and regional earthquakes to map the velocity variation of the upper mentle beneath the Alpine region. Techniques and codes used are the same as in the case of the previous work. The methodology, however, differs from the Dinarides tomography case in a sense, that while before we used many earthquakes and less stations pairs (due to sparser station coverage), for the Alps, we use less earthquakes (31) and many more stations pairs (tens of thousands; the region is also larger) making use of the dense station coverage of the AlpArray network.

We plan to calculate both Rayleigh and Love wave phase velocity dispersion curves, calculate lateral distribution for range of frequencies, assemble local dispersion curves and invert independently Rayleigh and Love phase velocities for shear-wave velocity distribution with depth. The two s_V and s_H models will allow to estimate depth-dependent radial anisotropy.

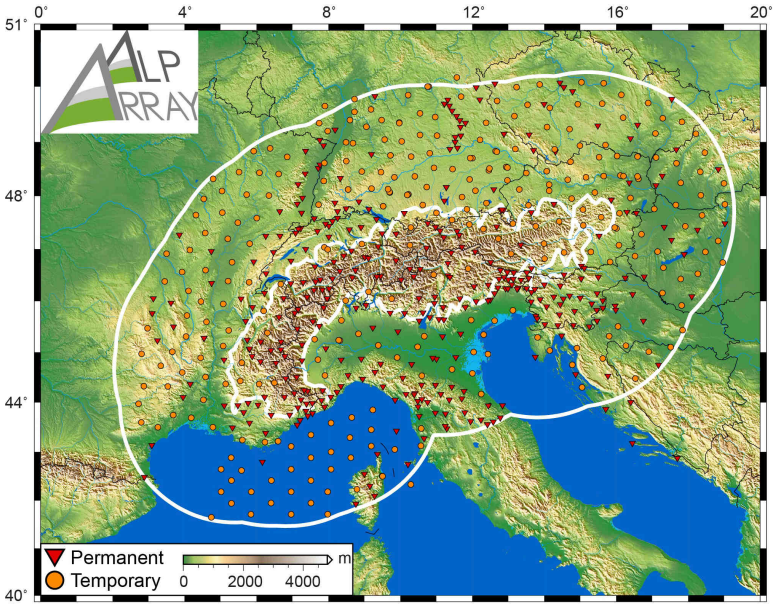

AlpArray region. Figure from Hetényi et al., 2018.

© Authors. All rights reserved

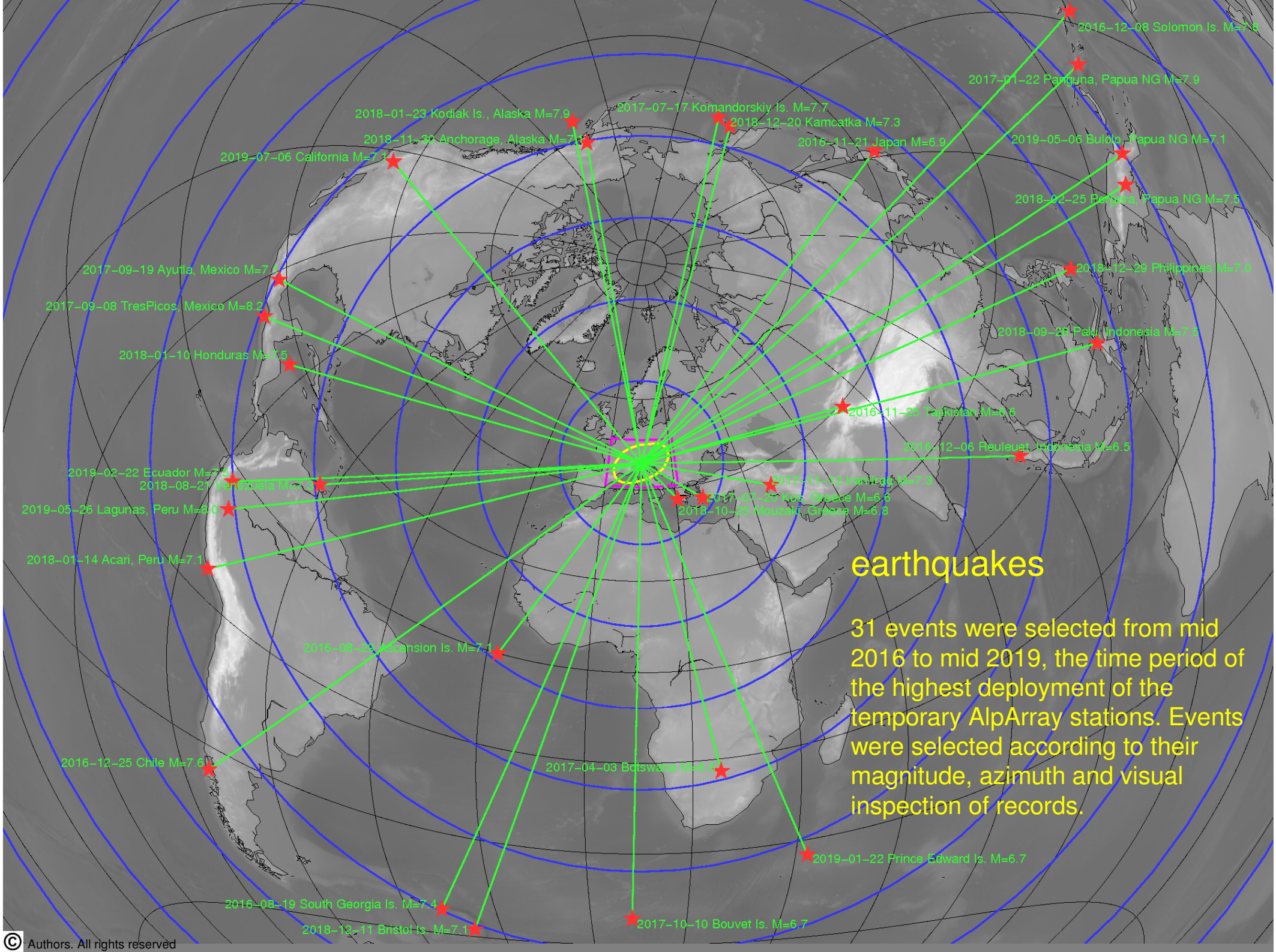

© Authors. All rights reserved

stations

we use **676** stations in the generalized AlpArray region, including OBS

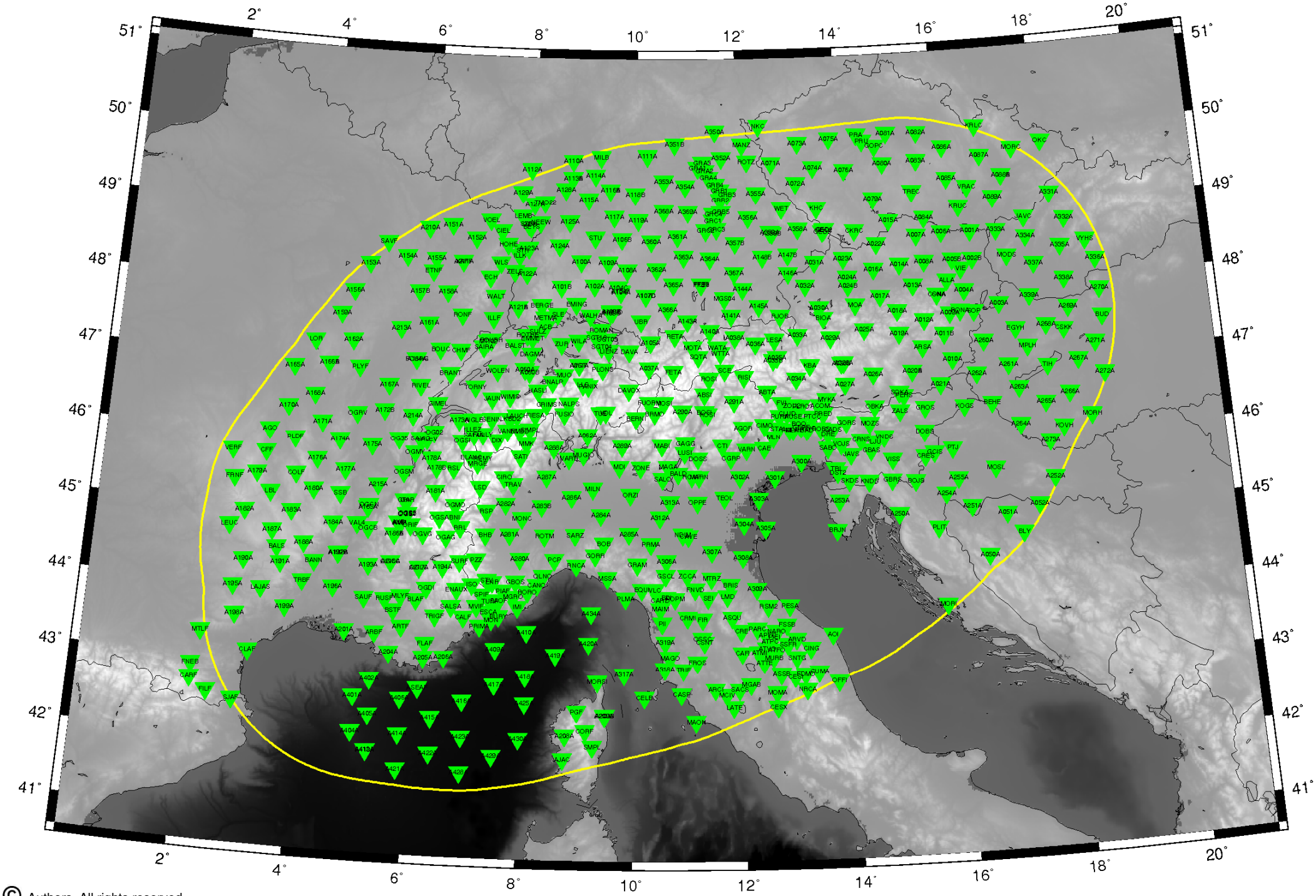

© Authors. All rights reserved

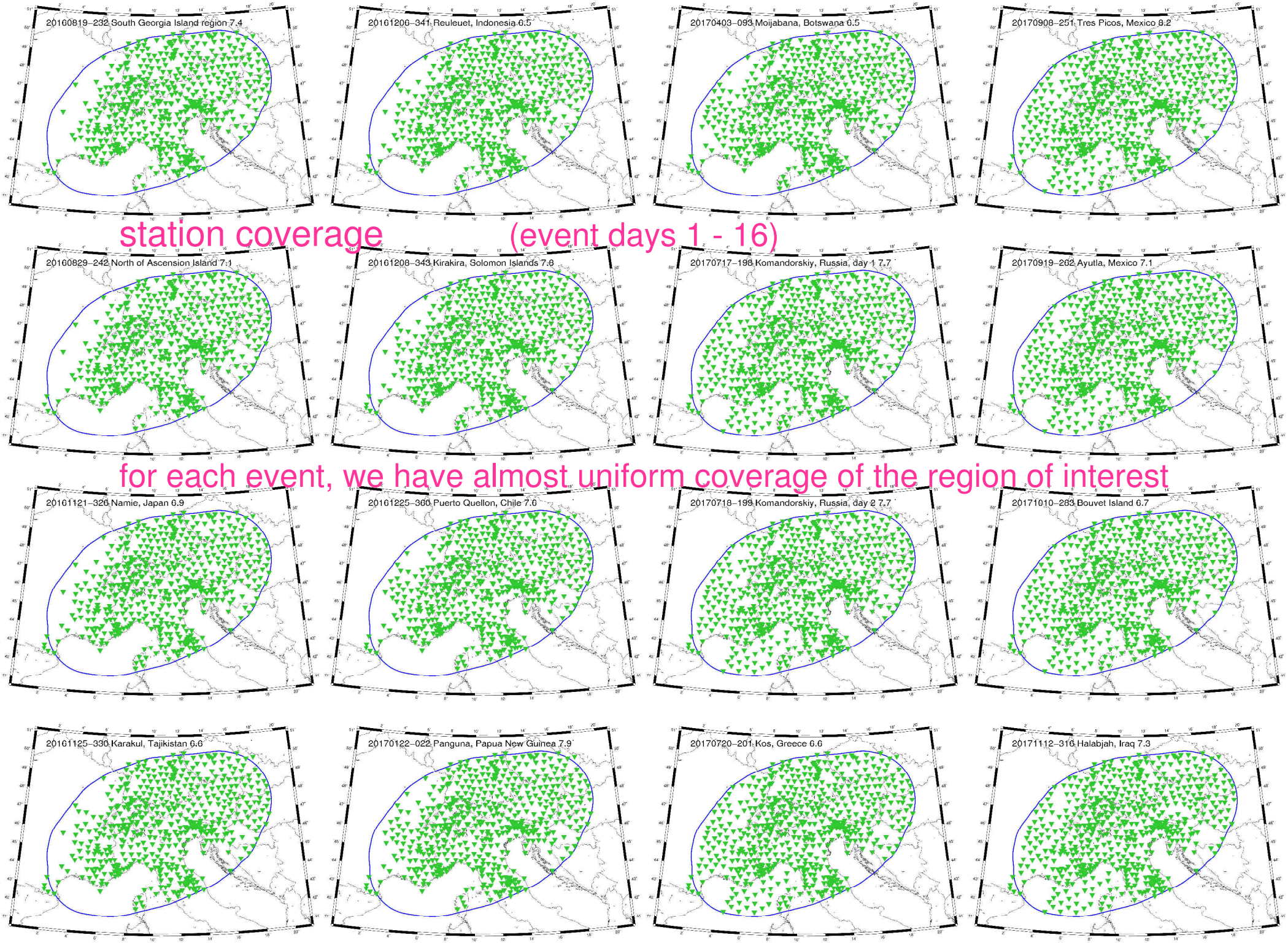

© Authors. All rights reserved

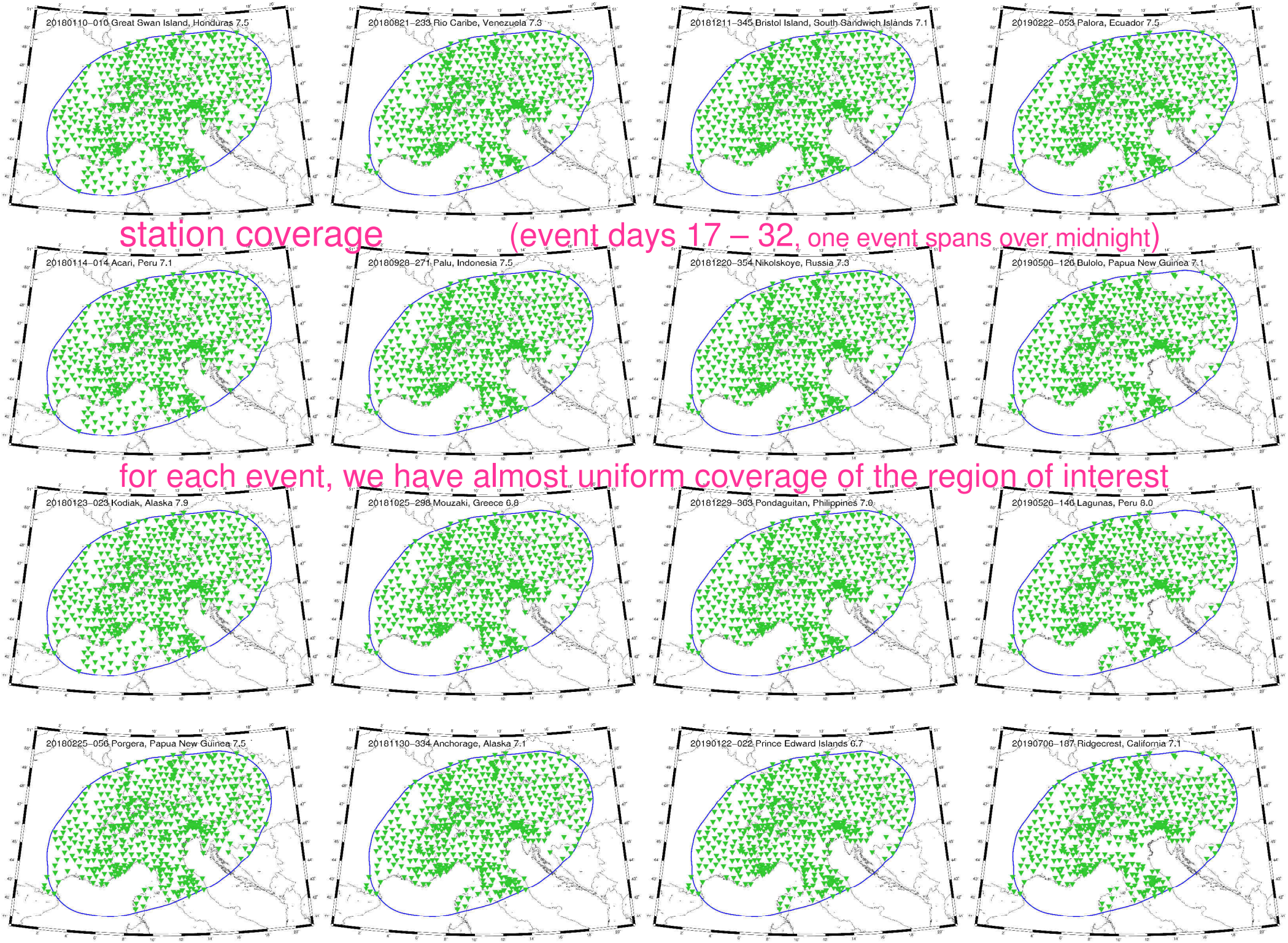

station coverage (event days 17 – 32, one event spans over midnight)

for each event, we have almost uniform coverage of the region of interest

© Authors. All rights reserved

data availability

orange bars:
number of records available for each event
average = 562

blue bars:
number of records after automatic data quality check
average = 537

For each event, we loose between 2.3% and 6.6% of records.

#	date	location	M
1	2016-08-19	South Georgia Island region	7.4
2	2016-08-29	North of Ascension Island	7.1
3	2016-11-21	Namie, Japan	6.9
4	2016-11-25	Karakul, Tajikistan	6.6
5	2016-12-06	Reuleuet, Indonesia	6.5
6	2016-12-08	Kirakira, Solomon Islands	7.8
7	2016-12-25	Puerto Quellon, Chile	7.6
8	2017-01-22	Panguna, Papua New Guinea	7.9
9	2017-04-03	Moijabana, Botswana	6.5
10	2017-07-17	Nikolskoye, Russia	7.7
11	2017-07-20	Kos, Greece	6.6
12	2017-09-08	Tres Picos, Mexico	8.2
13	2017-09-19	Ayutla, Mexico	7.1
14	2017-10-10	Bouvet Island region	6.7
15	2017-11-12	Halabjah, Iraq	7.3
16	2018-01-10	Great Swan Island, Honduras	7.5
17	2018-01-14	Acari, Peru	7.1
18	2018-01-23	Kodiak, Alaska	7.9
19	2018-02-25	Porgera, Papua New Guinea	7.5
20	2018-08-21	Rio Caribe, Venezuela	7.3
21	2018-09-28	Palu, Indonesia	7.5
22	2018-10-25	Mouzaki, Greece	6.8
23	2018-11-30	Anchorage, Alaska	7.1
24	2018-12-11	Bristol Island, South Sandwich Is.	7.1
25	2018-12-20	Nikolskoye, Russia	7.3
26	2018-12-29	Pondaguitan, Philippines	7.0
27	2019-01-22	Prince Edward Islands region	6.7
28	2019-02-22	Palora, Ecuador	7.5
29	2019-05-06	Bulolo, Papua New Guinea	7.1
30	2019-05-26	Lagunas, Peru	8.0
31	2019-07-06	Ridgecrest Earthquake Sequence	7.1

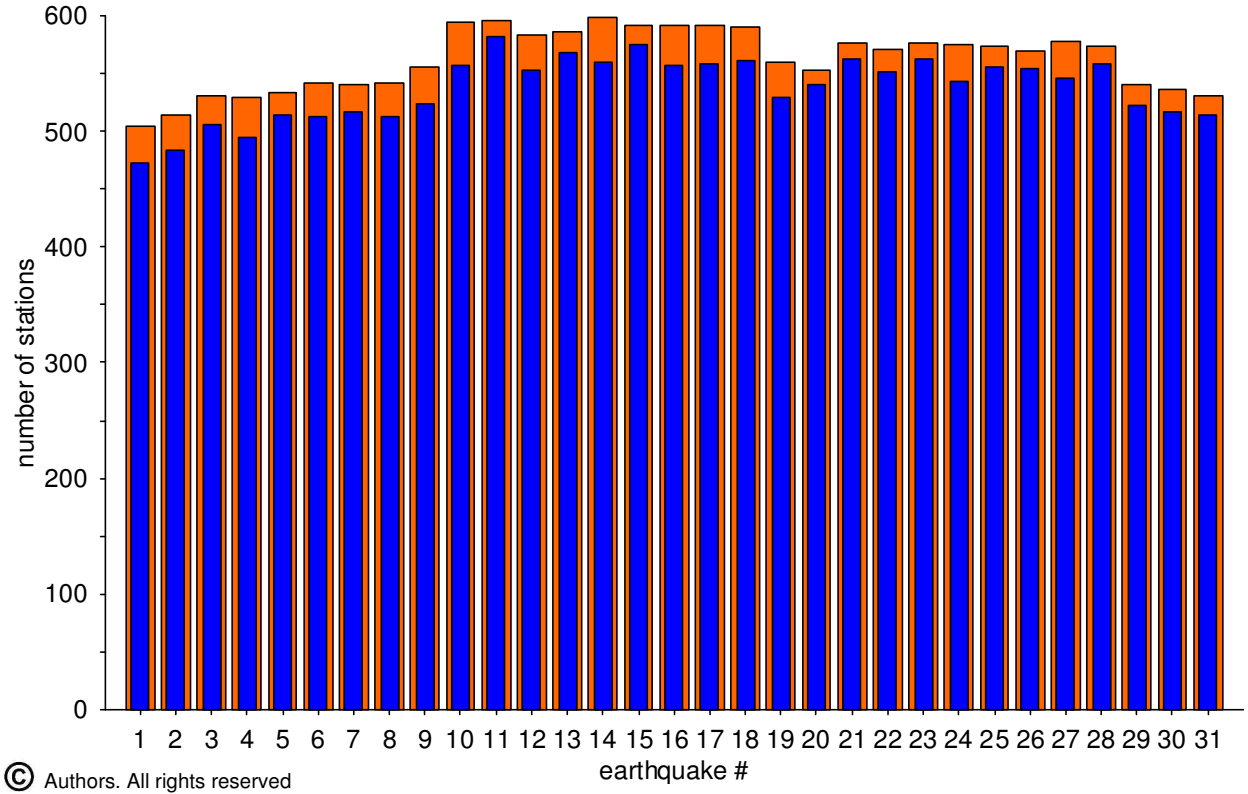

automatic DQ check removes records with:

- missing component
- zero traces
- too short traces
- gaps longer than 3 s
- number of traces higher than 20 per 1000s
- records with mutual amplitude ratio between components higher than 10

© Authors. All rights reserved

visual check of all components (examples 1)

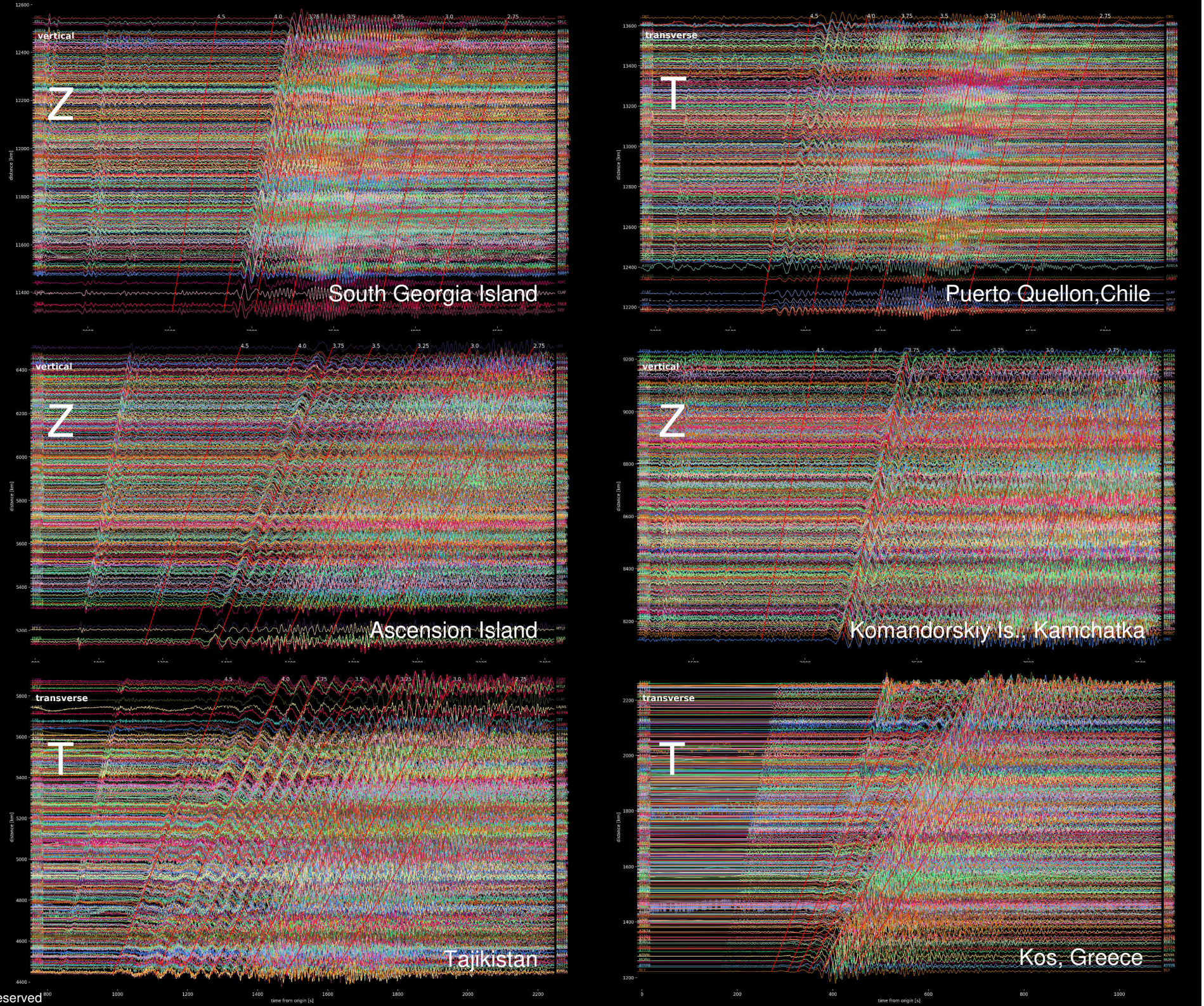

© Authors. All rights reserved

visual check of all components (examples 2)

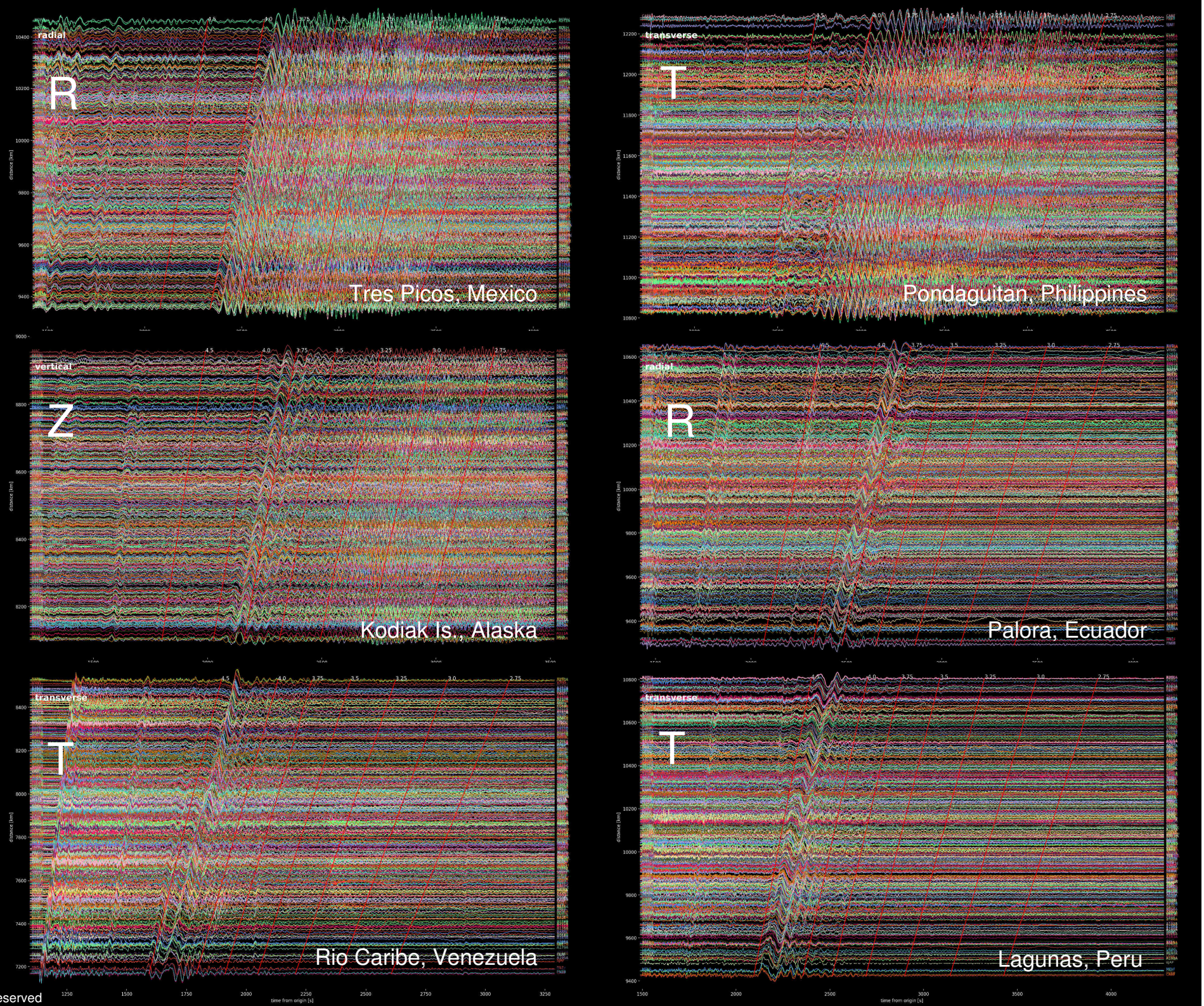

© Authors. All rights reserved

number of stations used

in addition to orange (available) and blue (good data quality), green bars show the number of stations used for the two-station measurement for each event

Σ of blue = 16662 records
=> on average 537 per event
Σ of green = 15155 records <=> 91% of blue

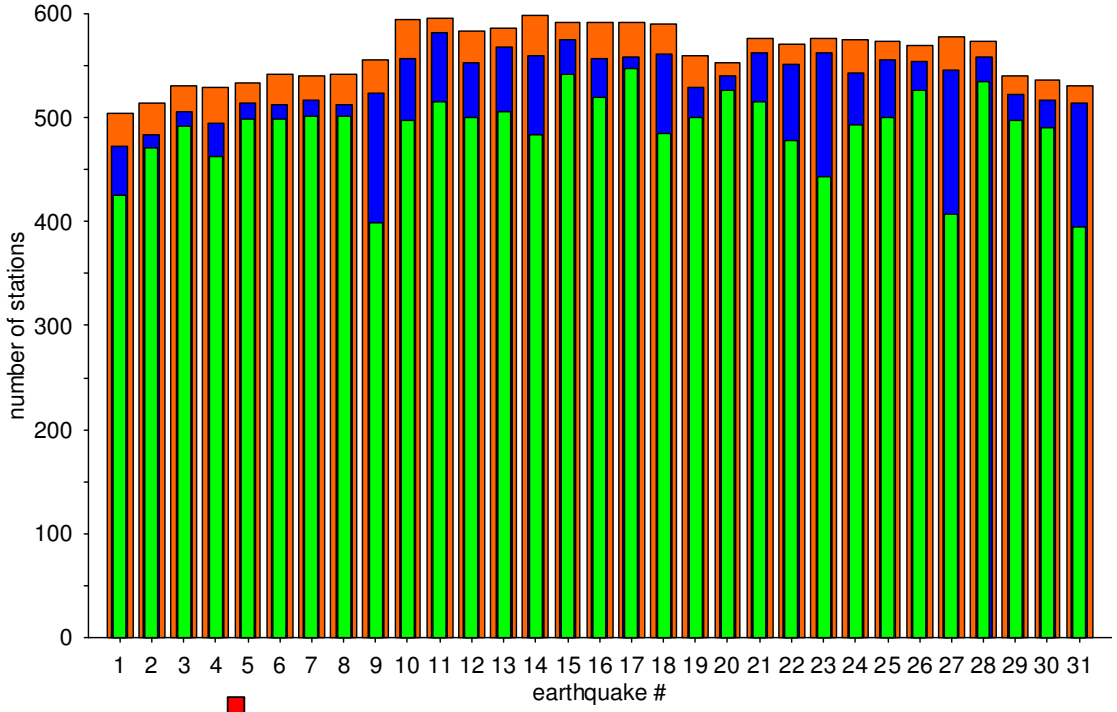

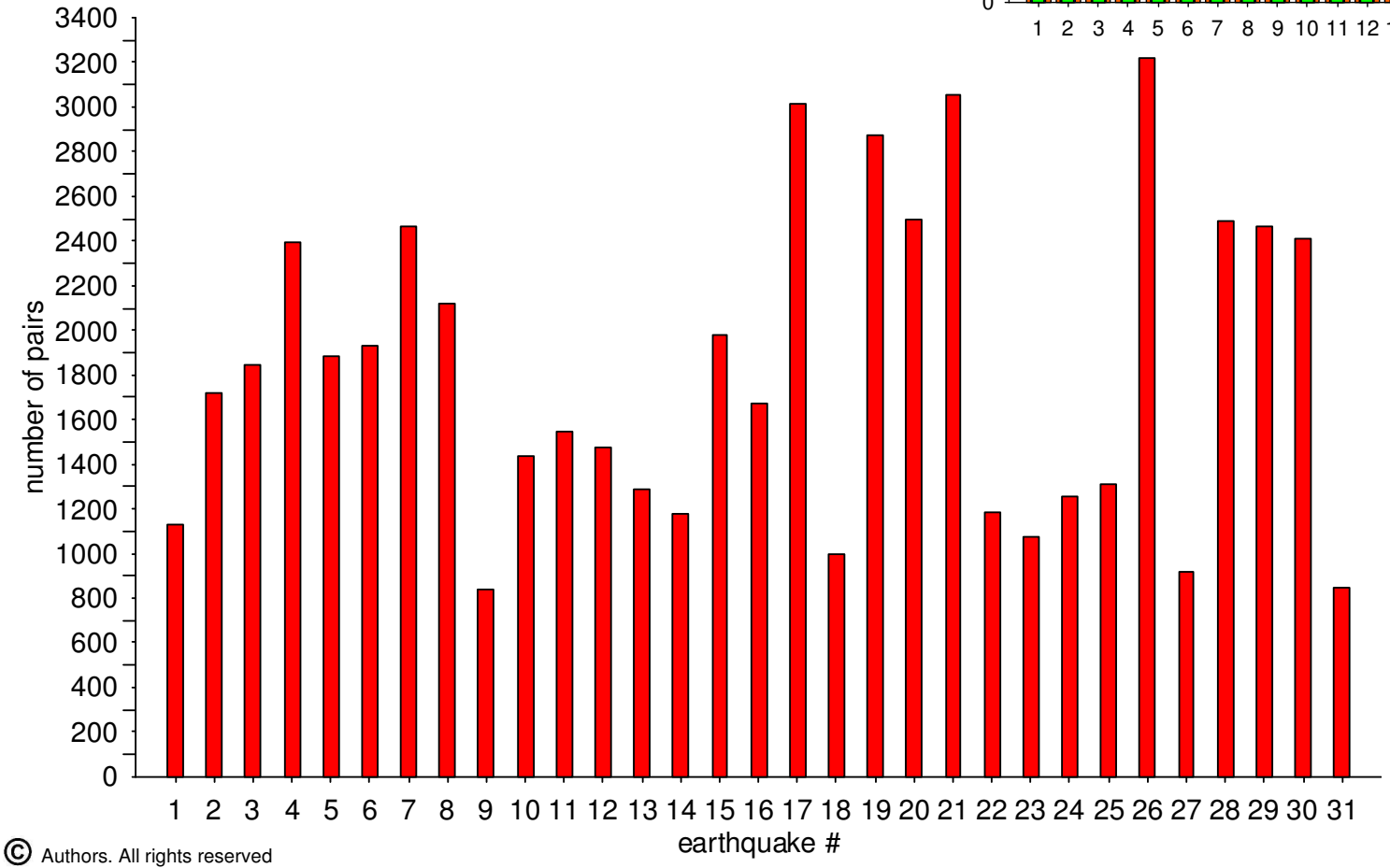

number of pairs

total pairs	56514
triplicate paths	821
duplicate paths	5637
single paths (=pairs)	42777

records in pairs
(2*56514 =) 113028

each record (green) is used
113028 / 15155 = 7.5 times
each record (blue) is used
113028 / 16662 = 6.8 times

© Authors. All rights reserved

coverage

42777 + 5637 + 821 = **49235** unique paths covering the Alpine region

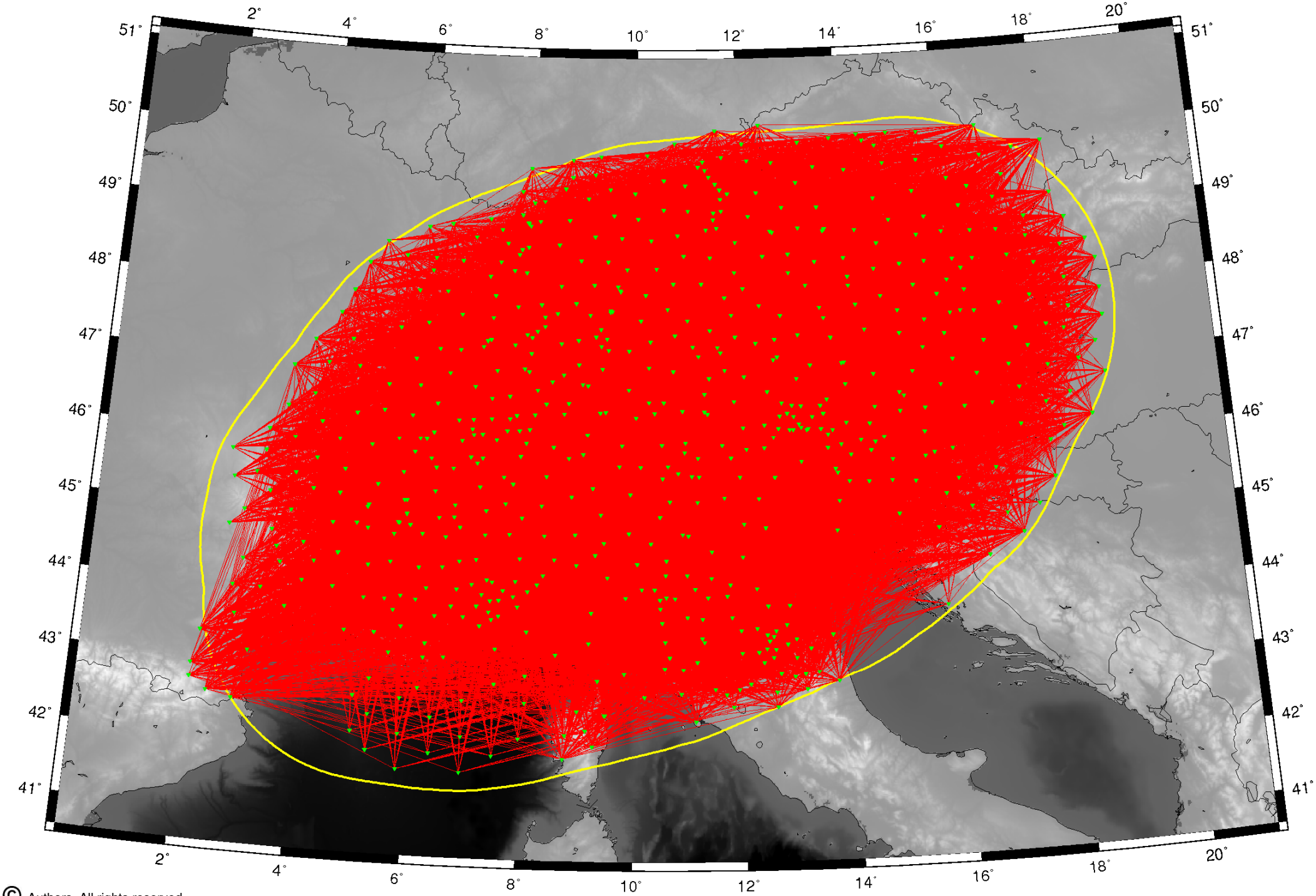

© Authors. All rights reserved

Thanks to the dense network of around 540 station, we are able to form thousands of two-station pairs for every single earthquake. From the methodology point of view, the main aim is to check, whether dense ray coverage of mostly single two-station measurement can replace sparser coverage with many measurement over the same path, as usually used in former studies. Moreover, in our approach, every record is used for several two-station profiles for each earthquake.

Tomography of the upper mantle beneath the Alps follows our study on the upper mantle beneath the Dinarides. There is an geographical overlap, which will allow to compare the two results.

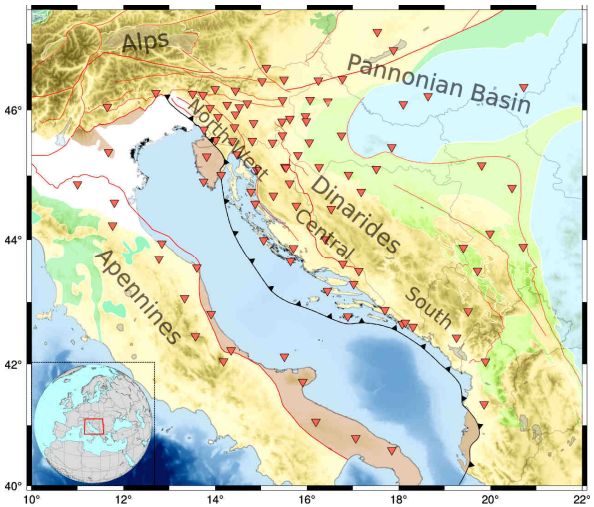

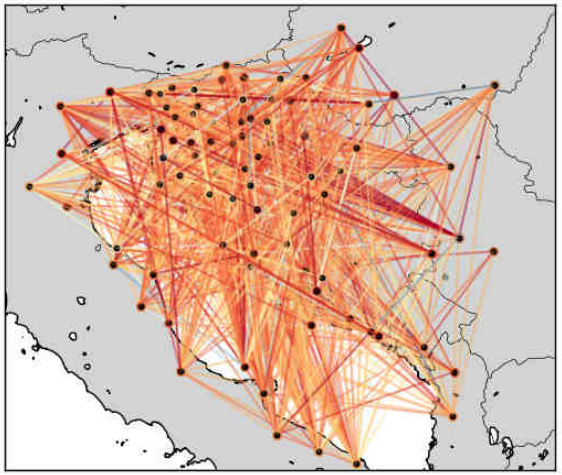

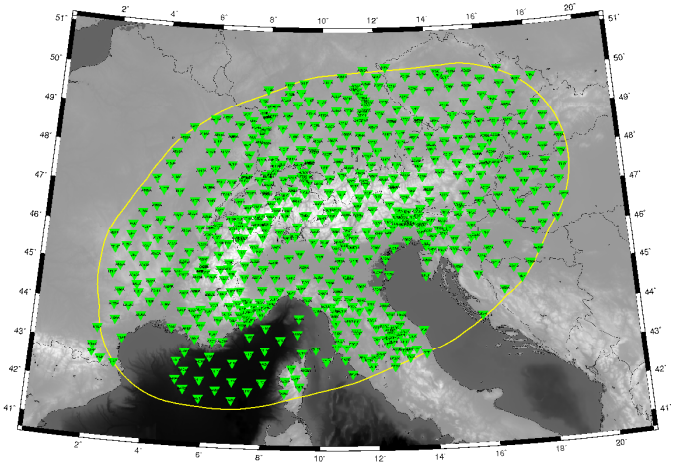

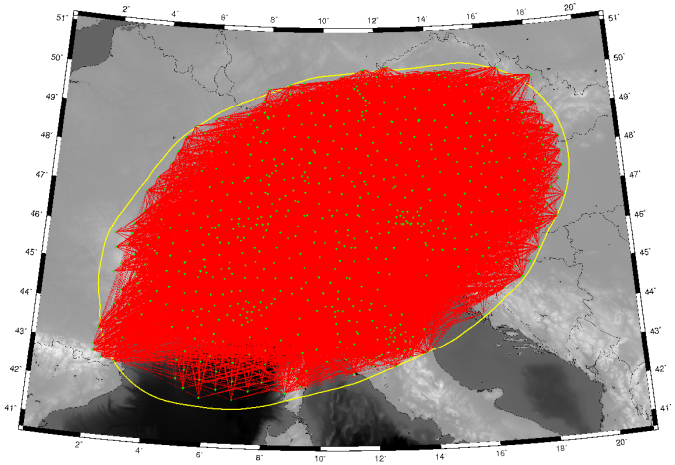

phase velocity maps of the Alps coming soon ...

© Authors. All rights reserved

petr.kolinsky@univie.ac.at

acknowledgements

Maps plotted using GMT by Wessel, P., Smith, W. H. F., Scharroo, R., Luis, J. F. and Wobbe, F., 2013: Generic Mapping Tools: Improved version released, EOS Trans. AGU, 94, 409-410.

Earthquake source parameters by U. S. Geological Survey.

Data from temporary stations by the AlpArray Working Group www.alparray.ethz.ch.

Data from permanent stations by national seismological services and ORFEUS-EIDA.

© Authors. All rights reserved